Kinetics of Nucleotide-Induced Changes in the Tryptophan Fluorescence of the Molecular Chaperone Hsc70 and Its Subfragments Suggest the ATP-Induced Conformational Change Follows Initial ATP Binding†

Jeung-Hoi Ha and David B. McKay*

Beckman Laboratories for Structural Biology, Department of Structural Biology, Stanford University School of Medicine, Stanford, California 94305

Received May 17, 1995; Revised Manuscript Received June 30, 1995®

ABSTRACT: The kinetics of nucleotide-induced changes of tryptophan fluorescence have been measured for recombinant bovine 70 kDa heat shock cognate protein (Hsc70), a 60 kDa subfragment (amino acid residues 1−554) which has ATPase and peptide binding activities, and a 44 kDa subfragment (residues 1−386) which has only ATPase activity. The fluorescence changes resulting from ATP binding to Hsc70 and the 60 kDa fragment are biphasic, and can be interpreted as arising from a two-step process in which ATP initially binds in a bimolecular reaction, followed by a conformational change of the protein−MgATP complex. Fluorescence changes resulting from ADP binding indicate a single-step, bimolecular process. Under single-cycle conditions of the ATPase reaction, a fluorescence change is observed whose rate constant correlates with product release in Hsc70, and with product release/ATP hydrolysis (which are kinetically indistinguishable under single-cycle conditions) in the 60 kDa fragment. These data support a scheme for Hsc70 in which a conformational transition is induced after initial ATP binding but prior to hydrolysis, and the reverse transition is induced by product release. The 60 kDa fragment shows behavior that is quantitatively similar to that of Hsc70. The 44 kDa ATPase fragment does not show biphasic kinetics for ATP binding, and does not show fluorescence changes that suggest conformational changes of the type seen in Hsc70 and the 60 kDa fragment.

Hsc70,[1] a molecular chaperone, is a constitutively-expressed member of the 70 kDa heat shock protein family. Hsc70 is thought to inhibit misfolding and aggregation of nascent polypeptides during translation, to facilitate transmembrane translocation of proteins targeted to specific organelles, and to target denatured proteins for lysosomal degradation *in vivo* [for reviews, see Gething and Sambrook (1992), McKay (1993); McKay et al. (1994), and Hightower et al. (1994)]. In addition, Hsc70 has been shown to accelerate the rate of uncoating of clathrin-coated vesicles *in vitro* (Schlossman et al., 1984; Chappell et al., 1986). All of these activities involve binding and release of unfolded or denatured polypeptides; peptide binding/release is tightly coupled to an ATPase activity, in a manner such that Hsc70 has a higher affinity for denatured proteins in the presence of MgADP than in the presence of MgATP. The observation that ATP induced peptide release from 70 kDa heat shock proteins, but nonhydrolyzable analogs failed to do so, originally led to the suggestion that ATP hydrolysis was required for peptide release (Schmid & Rothman, 1985; Liberek et al., 1991). More recently, the observation that dissociation of denatured proteins occurs more rapidly than ATP hydrolysis has raised the suggestion that ATP binding, rather than hydrolysis, releases peptides (Palleros et al., 1993; Prasad et al., 1994).

Bovine Hsc70 has 650 amino acid residues. It can be divided into at least two functional domains: ATPase activity is localized in the amino-terminal ~385 residues, and peptide binding activity is predominantly localized in the carboxy-proximal region from residues ~385 to 550 (Chappell et al., 1987; Wang et al., 1993). Stable fragments of recombinant bovine Hsc70 have been produced, including a 44 kDa fragment with peptide-independent ATPase activity (residues 1−386), and a 60 kDa fragment that has both ATPase and peptide binding activities (residues 1−554), as well as full-length Hsc70. The three-dimensional structure of the ATPase fragment has been solved (Flaherty et al., 1990); the three-dimensional structure of the remainder of the protein has yet to be reported [although the secondary structure of the peptide binding domain of rat Hsc70 was determined by NMR (Morshauser et al., 1995)].

The reaction pathway and the rates of the individual steps of the ATPase cycle for peptide-free recombinant bovine Hsc70 and its 44 kDa fragment have been determined (Ha & McKay, 1994). The kinetic data are consistent with a four-step ATPase cycle, with ordered product release (P_i leaving before ADP), for both Hsc70 and its 44 kDa fragment (Scheme 1) (where E = Hsc70 or its subfragments). For Hsc70, ATP hydrolysis and P_i release are both relatively slow steps ($k_2 = 0.0030\ s^{-1}$ and $k_3 = 0.0038\ s^{-1}$ at 25 °C), while ADP release is significantly more rapid ($k_4 = 0.029\ s^{-1}$). The kinetic experiments that led to this scheme monitored only the substrate and products of the ATPase reaction; they did not attempt to monitor, either directly or indirectly,

† Supported by NIH Award GM-39928 to D.B.M.

* Author to whom correspondence should be addressed at the Department of Structural Biology, Sherman Fairchild Building, Stanford University School of Medicine, Stanford, CA 94305-5400.

® Abstract published in *Advance ACS Abstracts,* August 15, 1995.

[1] Abbreviations: Hsc70, 70 kDa heat shock cognate protein; kDa, kilodalton(s); P_i, orthophosphate; AMP-PNP, adenosine 5′-(β,γ-imidotriphosphate); Tris, 2-amino-2-(hydroxymethyl)-1,3-propanediol; HEPES, *N*-(2-hydroxyethyl)piperazine-*N*′-2-ethanesulfonic acid; Mg(OAc)$_2$, Mg(CH$_3$COOH)$_2$; mantATP, 2′(3′)-*O*-(*N*-methylanthraniloyl)-adenosine 5′-triphosphate; ϵATP, 1,N^6-ethenoadenosine triphosphate.

0006-2960/95/0434-11635$09.00/0

Scheme 1

$$E + ATP \underset{k_{-1}}{\overset{k_1}{\rightleftharpoons}} E\text{–}ATP \xrightarrow{k_2} E\text{–}ADP\text{–}P_i \underset{k_{-3}}{\overset{k_3}{\rightleftharpoons}}$$

$$E\text{–}ADP + P_i \underset{k_{-4}}{\overset{k_4}{\rightleftharpoons}} E + ADP + P_i$$

different conformational states of the proteins.

Solution small-angle X-ray scattering (SAXS) studies (Wilbanks et al., 1995) have identified two distinct conformational states for both Hsc70 and the 60 kDa fragment on the basis of differences in radii of gyration (R_g). Steady-state measurements in the presence of excess nucleotide demonstrate that one state correlates with the presence of MgADP, nonhydrolyzable ATP analogs, or MgATP with ~0.1 M Na^+ as a monovalent counterion, while the other state is induced by MgATP with ~0.1 M K^+. Upon mixing stoichiometric amounts of nucleotide-free protein and ATP, the transition to the ATP-induced R_g value occurs more rapidly than hydrolysis, and is complete by the time the first data point is collected, during the first 1−2 min of the reaction. The rate of the reverse transition, to the R_g seen in the presence of ADP, is slower than ATP hydrolysis, and is at least as slow as the rate of product release in the cycle.

Steady-state measurements of the fluorescence of the single tryptophan residue of DnaK, a 70 kDa heat shock protein found in *Escherichia coli*, have shown differences in emission spectra taken in the presence of ATP, presence of ADP, or absence of nucleotide (Palleros et al., 1992). It has been suggested that the differences in fluorescence monitor different conformational states of DnaK. Hsc70 has two tryptophan residues, at positions 90 in the ATPase domain and 580 in the carboxy-terminal region. In this work, we report the kinetics of nucleotide-induced changes in tryptophan fluorescence intensity for Hsc70, the 60 kDa fragment, and the 44 kDa ATPase fragment, using both stopped-flow mixing to measure changes on a rapid (approximately millisecond) time scale that was inaccessible in the SAXS experiments and conventional techniques to measure changes on a time scale similar to that of the SAXS experiments (approximately minutes). We suggest the differences in tryptophan fluorescence that we observe may monitor different conformations of Hsc70 and its subfragments, and we correlate these changes with steps in the ATPase cycle.

MATERIALS AND METHODS

Protein Expression and Purification. Recombinant wild-type Hsc70, the 44 kDa ATPase fragment, and the 60 kDa fragment were expressed in *E. coli* and purified to >95% homogeneity as described (O'Brien & McKay, 1993; Wilbanks et al., 1994; Wilbanks et al., 1995). The purified proteins were free of *E. coli* DnaK as judged by Western blot. Proteins were rendered nucleotide-free prior to experiments by methods described previously (Ha & McKay, 1994). Protein concentration was determined from the optical absorbance at 280 nm using extinction coefficients of 3.08×10^4 (M^{-1} cm^{-1}) for Hsc70, 2.37×10^4 (M^{-1} cm^{-1}) for the 60 kDa fragment, and 1.86×10^4 (M^{-1} cm^{-1}) for the 44 kDa fragment, calculated from the amino acid compositions (Genetic Computer Group programs, Madison, WI). Four different preparations of Hsc70 and two preparations each of the 44 kDa and 60 kDa fragments were used to assess reproducibility of results from different samples.

Adenine Nucleotides. ATP, ADP, and AMP-PNP were purchased from Sigma (St. Louis, MO). Nucleotide stock solutions prepared in double-distilled H_2O were neutralized to pH 7.0 with Tris base and stored at −20 °C.

Fluorescence Measurements. All experiments were carried out in 40 mM HEPES, 4.5 mM $Mg(OAc)_2$, and 75 mM KCl, adjusted to pH 7.0 with KOH at 25 °C, unless otherwise stated; this is referred to as KCl buffer. Some measurements were done in 40 mM HEPES, 4.5 mM $Mg(OAc)_2$, and 75 mM NaCl, adjusted to pH 7.0 with NaOH at 25 °C; this is referred to as NaCl buffer.

Rapid kinetic experiments (≤200 s) were performed on a Bio DX-17MV sequential stopped-flow ASVD spectrofluorometer (Applied Photophysics Ltd., Leatherhead, U.K.) equipped with a 150 W xenon arc lamp. To observe tryptophan fluorescence, an excitation wavelength $\lambda_{ex} = 290$ nm (1−2 mm slit width) was used; emitted radiation was selected with a SWG305 cutoff filter (CVI Laser, Albuquerque, NM) for Hsc70 and for the 60 kDa fragment, and with a WG320 cutoff filter (Applied Photophysics Ltd.) for the 44 kDa fragment. The experiment was initiated by rapidly mixing equal volumes of protein solution and nucleotide solution which had been preincubated at the desired temperature for at least 5 min. The dead time of the stopped-flow instrument, determined as described in Tonomura et al. (1978), was 2 ms. An instrumental time constant was fixed at less than or equal to 0.5% of the half-time of the fastest reaction. In the following discussion, the concentrations reported for proteins and nucleotides were those in the optical cell after mixing and dilution. The final concentration of proteins used in fluorescence measurement was 2.5 μM for Hsc70 and the 60 kDa fragment and 4.4 μM for the 44 kDa fragment.

Slow kinetic experiments (up to 30 min) were performed on an Aminco-Bowman Series2 luminescence spectrometer (SLM-Aminco, Urbana, IL) or on an SLM 8000C spectrofluorometer (SLM-Aminco). Samples were stirred continuously and thermostated. The tryptophan fluorescence of Hsc70 was monitored at 305 or 320 nm (both 8 nm band-pass) with excitation at 295 nm (1 nm band-pass). The fluorescence of the 60 kDa fragment was observed through a 335 nm filter with excitation at 290 nm (4 nm band-pass). In some samples, long-term drift of the fluorescence base line was observed; it was found this could be prevented by siliconizing the cuvette with 5% dichlorodimethylsilane in hexane. Protein solution (1.3 mL of 2.5 μM) was preincubated at 25 °C for 10 min, and the reaction was initiated by addition of 1 μL of ATP stock solution equilibrated at room temperature. The final concentration of ATP was 2.1 μM. The time required for manual mixing was ≤15 s.

Stopped-flow kinetic data were analyzed using the nonlinear least-squares program supplied by Applied Photophysics. KleidaGraph was used to analyze the slow kinetics data. The uncertainty reported is the standard error of a least-squares fit.

RESULTS

Changes in the Tryptophan Fluorescence of Hsc70 and Its Subfragments upon Adenine Nucleotide Binding. To test

whether interaction with adenine nucleotides results in changes in fluorescence, steady-state emission spectra (λ_{ex} = 290 nm) were collected for Hsc70, the 60 kDa fragment, and the 44 kDa fragment, and spectra recorded in the presence of excess ATP or ADP were compared to those recorded in absence of nucleotide. The maximum differences between fluorescence intensitites of nucleotide-bound and nucleotide-free protein were found in the wavelength range 300−330 nm; the relative changes ranged from 4 to 15% in magnitude. The steady-state spectra were used as a guide for selecting cutoff filters for stopped-flow experiments and band-pass filters or emission wavelength for slow kinetic experiments.

The fluorescent ATP analogs mantATP and ϵATP were also tested to see whether they showed a larger fluorescence change than tryptophan. No change in mantATP fluorescence was observed when it was mixed with nucleotide-free Hsc70 (data not shown). Mixing Mg-ϵATP with Hsc70 resulted in decreased fluorescence of the nucleotide, but the amplitude was much smaller than the intrinsic tryptophan fluorescence change (data not shown). In addition, the kinetics of the ϵATP fluorescence change were similar to those observed upon binding of MgADP, suggesting that Mg-ϵATP binding mimics that of MgADP.

Changes in Fluorescence from MgADP Binding to Hsc70. Stopped-flow measurements show that addition of MgADP to nucleotide-free Hsc70 at 25 °C results in a decrease in fluorescence intensity (Figure 1a). When Hsc70 is combined with an equal volume of buffer, no change in fluorescence is observed (Figure 1b), indicating that the change is due to nucleotide binding. The intensity change reaches completion in less than 0.2 s and can be fit with a single exponential. A similar behavior was observed at 18.5 °C (data not shown). The rate of change of fluorescence intensity was measured at 25 °C as a function of [ADP] (Figure 1c). The larger errors at higher [ADP] correlate with the more rapid (and hence, larger in magnitude) decay times; the relative errors (i.e., errors as a percentage of the average value) are similar for measurements at different nucleotide concentrations. The observed rate constant (k_{obs}), determined over the [ADP] range 32−218 μM, increases linearly with increasing [ADP], showing qualitatively that the change in fluorescence results from a second-order, or bimolecular, process.

Theoretically, the slope of the linear fit to k_{obs} versus [ADP] yields the bimolecular association rate constant (k_{-4} of Scheme 1), and the intercept yields the dissociation rate constant (k_4). Fitting a straight line to the data in Figure 1c yields a value of (1.1 ± 0.1) × 10^6 M^{-1} s^{-1} for the slope and −1.8 ± 13 s^{-1} for the intercept. Previously we reported results from filter binding experiments showing that dissociation of MgADP from Hsc70 at 25 °C has a rate constant 0.0288 ± 0.0018 s^{-1} (Ha & McKay, 1994). This value is small compared to the range of measured values of k_{obs} from the fluorescence experiment, and agrees within experimental error with the value determined for the intercept. In this context, an alternative method of linear fit is to fix the intercept to 0.0288 s^{-1}; when this is done, the slope of the line is again (1.1 ± 0.1) × 10^6 M^{-1} s^{-1}, equal to the value computed when the intercept is a floating parameter in the fit. Although the statistical error of the fit is only ~10%, inspection of the spread of measured values and errors for k_{obs} shows deviations of ~±50% from the best-fit line, suggesting that the statistical error of the linear fit understates

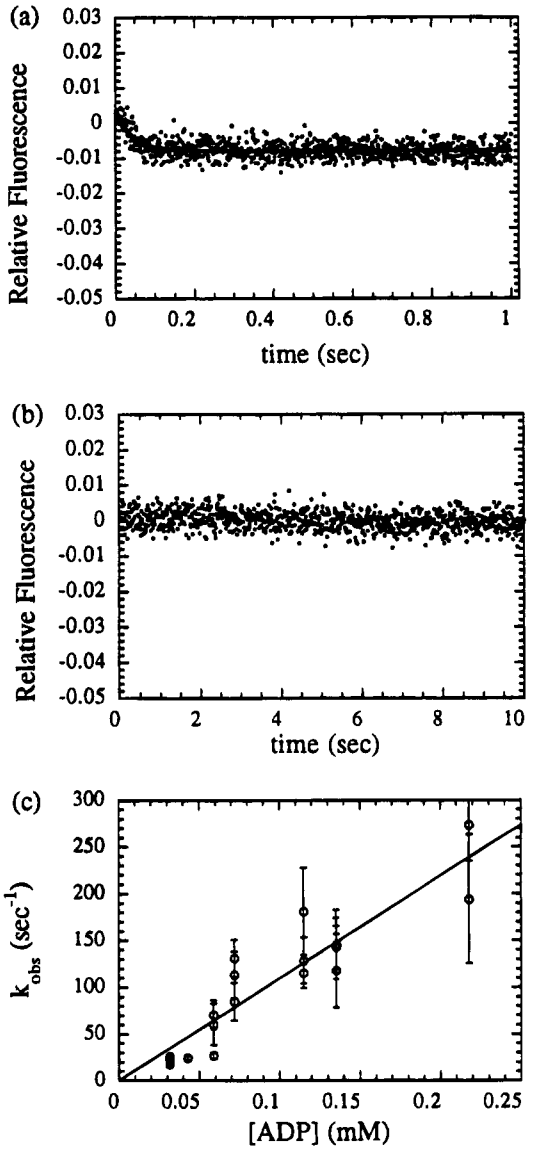

FIGURE 1: Change in tryptophan fluorescence of Hsc70 at 25 °C when ADP binds. (a) Monitored over 1.0 s after the rapid mixing with 32 μM ADP. Curve represents a nonlinear least-squares fit of a single exponential to fluorescence signals with the observed rate constant, k_{obs} = 22.4 ± 2.1 s^{-1}. (b) Fluorescence of Hsc70 was monitored over 10 s after the rapid dilution with an equal volume of KCl buffer at 25 °C. (c) Plot of k_{obs} determined at 25 °C as a function of the concentration of ADP. The line is the result of a least-squares linear fit to the data.

the uncertainty in the accuracy of the slope. The bimolecular association rate of MgADP measured by stopped-flow fluorescence can be compared to the value determined by filter binding, (0.41 ± 0.05) × 10^6 M^{-1} s^{-1} (Ha & McKay 1994).

Changes in Fluorescence from MgATP Binding to Hsc70. When MgATP is mixed with Hsc70 in KCl buffer, the change in fluorescence is biphasic. At 18.5 °C, the initial, rapid phase levels off in <0.2 s (Figure 2a), while the second phase has a characteristic decay time of the order ~5 s (Figure 2b). Using data collected at 18.5 °C as a test, two methods were examined to extract rate constants from the data. First, the fluorescence intensity versus time was parameterized with two exponentials by (1) fitting data in the time range 0.0−0.2 s with a single exponential and, separately, (2) fitting data in the time range 0.2−20.0 s with

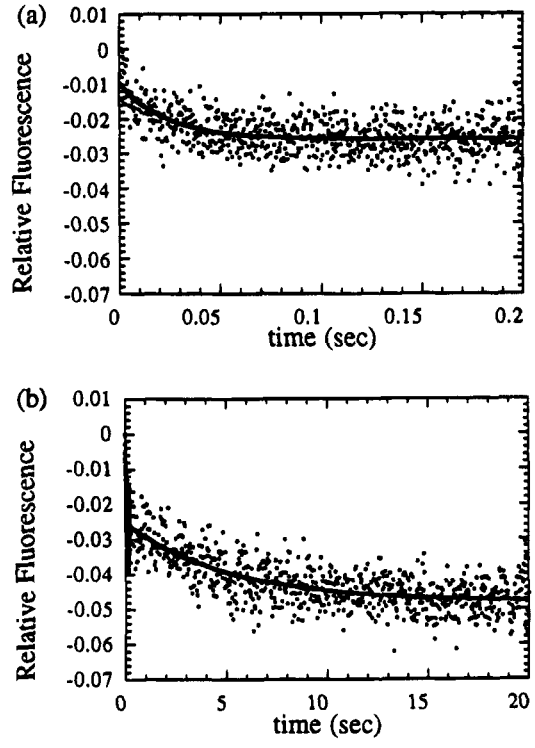

FIGURE 2: Change in tryptophan fluorescence of Hsc70 at 18.5 °C when ATP binds. (a) Monitored over 0.2 s after the rapid mixing with 74 μM ATP. Curve represent a nonlinear least-squares fit of a single exponential to fluorescence signals with the observed rate constant of the fast phase, $k_\alpha = 43.0 \pm 4.7\ s^{-1}$. (b) Monitored over 20 s after the rapid mixing with 74 μM ATP. Curve represent a nonlinear least-squares fit of a single exponential to fluorescence signals with the observed rate constant of the slow phase, $k_\beta = 0.19 \pm 0.01\ s^{-1}$.

a single exponential. Second, a single function with two exponential terms was fit over the entire range 0.0−20.0 s. The rate constants calculated using the two procedures agree within error. We subsequently used the first procedure for data analysis when one phase amplitude of the two was too small for an accurate determination of the rate constant. Measurements as a function of [ATP] over a range of 74−550 μM show that the rate constant of the initial, rapid, phase (which we denote k_α) increases linearly with [ATP]. The slope of the linear fit to the observed value of k_α versus [ATP] (=the ATP association rate k_1 of Scheme 1) equals $(4.2 \pm 0.5) \times 10^5\ M^{-1}\ s^{-1}$. Over the same [ATP] range, the rate constant of the second, slower, phase (which we denote k_β) is independent of nucleotide concentration (Figure 3a). The average value of k_β at 18.5 °C is $0.15 \pm 0.01\ s^{-1}$. MgATP binding to Hsc70 therefore is not a single-step bimolecular association reaction. Instead, it takes place in at least two steps: (1) a bimolecular association of MgATP with Hsc70, and (2) a step which theoretically could be either a conformational change of a Hsc70−MgATP complex after nucleotide binding, a first-order conformational change of Hsc70 prior to nucleotide binding, or a competition between two different ATP binding modes with Hsc70. We consider each of these alternatives under Discussion; we will state at this point that we favor the model of ATP binding first, followed by a conformational change of the Hsc70−ATP complex.

We determined the dependence of k_1 (the ATP "on" rate) and k_β on temperature. [The pH of the KCl buffer would vary approximately among 6.7−7.2 over the temperature of

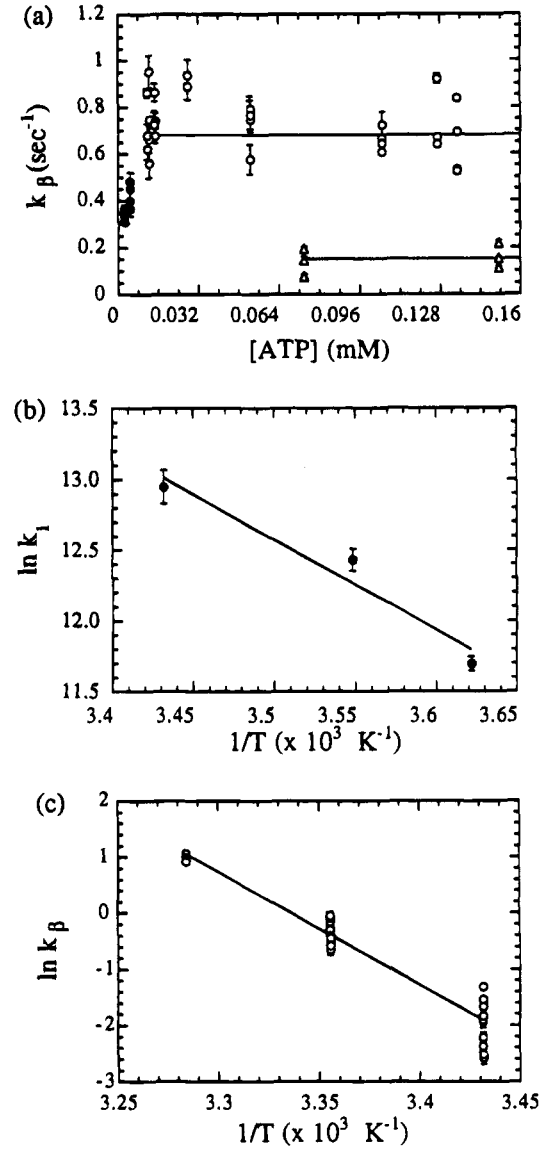

FIGURE 3: Temperature dependence of rate constants of fluorescence changes of Hsc70 when ATP binds. (a) Plot of k_β determined at 18.5 and 25 °C as a function of the concentration of MgATP. (△) 18.5 °C and (○) 25 °C; under the pseudo-first-order condition; (●) 25 °C when the concentration of MgATP is less than 5 times the Hsc70 concentration; this is a concentration range where the approximation of pseudo-first-order kinetics no longer holds and analysis with a single exponential is therefore oversimplification. Lines represent the average value of k_β determined over the ATP concentration range 12.5−450 μM at 25 °C and 74−550 μM at 18.5 °C. (b) Arrhenius plot of the apparent bimolecular association rate constant, k_1. (c) Arrhenius plot of the rate constant of the slow phase, k_β.

3−37 °C (Perrin & Dempsey, 1974). The effect of pH changes of this magnitude on the rate constants, due to the temperature dependence of the pK_a of HEPES, is likely to be minimal and has been ignored.] The amplitudes, as well as the rates, of the observed fluorescence changes are temperature-dependent (cf. Figure 6a). In particular, at $T \geq 25$ °C, the amplitude of the initial fast phase is too small to allow accurate determination of k_α. Consequently, measurements of k_α were made for temperatures between 3.1 and 18.5 °C, over a range 74−550 μM in [ATP]. k_α increases linearly with increasing [ATP] at $T < 18$ °C, similar to what was observed at 18.5 °C. The resulting Arrhenius plot of ln k_1 versus $1/T$ gives a straight line (Figure 3b), and

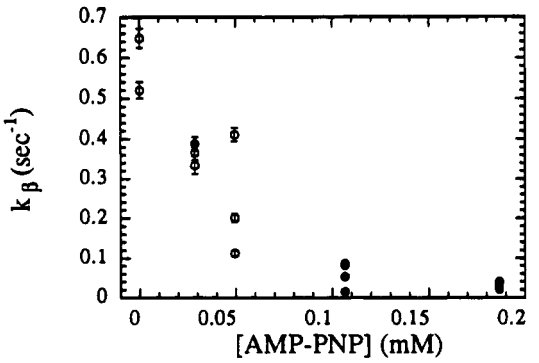

FIGURE 4: Association kinetics of ATP at 17 μM with Hsc70 as a function of the concentration of AMP-PNP at 25 °C. Hsc70 was rapidly mixed with nucleotide solution containing 17 μM ATP and various amounts of AMP-PNP, and the apparent rate constant of fluorescence change was calculated from a fit of a single exponential decay to fluorescence.

the slope of the plot estimates the activation energy of this step as 12.7 ± 3.0 kcal mol^{-1}. Extrapolation gives an estimate for k_1 of ~7 × 10^5 M^{-1} s^{-1} at 25 °C.

Measurements of the rate of the second phase were made over the [ATP] range 74−550 μM at 18.5 °C, 2.5−450 μM at 25 °C, and 127−259 μM at 31.5 °C. The amplitude of the slow phase is too small to determine k_β accurately at T < 18.5 °C. The rate constant k_β is independent of [ATP] at concentrations >10 μM (Figure 3a). The average value of k_β at 25 °C is 0.68 ± 0.02 s^{-1}; at 31.5 °C, it is 2.7 ± 0.1 s^{-1}. An Arrhenius plot of the second step is also linear (Figure 3c); the slope of the plot is 40 ± 1 kcal mol^{-1}.

Similar stopped-flow fluorescence experiments were carried out to determine the effects of MgATP binding in NaCl buffer at 25 °C. Under these conditions, the kinetics of the fluorescence change are monophasic, and the rate constant, derived from fitting a single exponential to fluorescence versus time, increases linearly with increasing [ATP] (27−245 μM). The slope of the linear fit to the rate versus [ATP] yields the bimolecular association rate constant (4.3 ± 0.2) × 10^5 M^{-1} s^{-1} when the intercept is fixed to zero; the same value is obtained when the intercept is included as a variable parameter in the fit, in which case it is estimated to be 1.2 ± 4.6 s^{-1}.

Changes in Fluorescence from MgAMP-PNP Binding to Hsc70. The nonhydrolyzable ATP analog AMP-PNP has been shown to bind bovine Hsc70, and to compete with ATP with approximately 2 orders of magnitude weaker affinity (Gao et al., 1994). Initially, we examined the effect of mixing AMP-PNP alone with nucleotide-free recombinant Hsc70 at 25 °C. No significant change in fluorescence was observed over a time span of 200 s and a [AMP-PNP] range of 65−932 μM.

Next we examined the effect of AMP-PNP on the rate of fluorescence change induced by ATP binding at 25 °C. Hsc70 was rapidly mixed with a mixture of ATP and AMP-PNP; [ATP] was held constant at 17 μM, and [AMP-PNP] was varied over the range 0−186.5 μM. Under these conditions, the first step of ATP binding is much more rapid than the second, since k_1[ATP] ~ 12 s^{-1} ≫ 0.68 s^{-1}. The rate and amplitude of the slower phase of the fluorescence change were monitored. The amplitude remained approximately constant over the entire range of [AMP-PNP] tested, while the rate decreased with increasing [AMP-PNP] (Figure 4). This suggests that AMP-PNP competes with ATP for binding, and further corroborates the suggestion that the observed fluorescence changes are due to specific nucleotide binding.

Rate of Dissociation of ADP from Hsc70 Estimated from Fluorescence. Since MgATP binding generates a larger fluorescence signal change than MgADP binding, the effect of displacement of ADP from Hsc70 by ATP can be monitored. To check the correlation between the fluorescence experiments reported here and the results of kinetic experiments reported previously, we have monitored the consequence of ADP release to determine its dissociation rate. Starting with a Hsc70−MgADP complex, if ATP is added in substantial molar excess over the complex (so that k_1[ATP]$_{free}$ ≫ k_{-4}[ADP]$_{free}$, and ATP will replace ADP when it dissociates), and if the binding steps of ATP are more rapid than the release rate of ADP (k_α, k_β ≫ k_4 of Scheme 1), then ADP dissociation will be the rate-limiting step of the nucleotide exchange process. The rate of change of fluorescence after rapid mixing of 425 μM MgATP with 2.5 μM Hsc70−MgADP complex followed a single exponential (data not shown) and yielded an apparent ligand exchange rate constant of 0.022 ± 0.002 s^{-1} at 25 °C. This estimation of the MgADP dissociation rate is in good agreement with the value determined by filter binding, 0.0288 ± 0.0018 s^{-1} (Ha & McKay, 1994).

Previously we showed that ADP dissociation from Hsc70 is retarded by high [P_i], presumably as a result of ordered product release (Ha & McKay, 1994). To further test the correlation between previous kinetic experiments and results from fluorescence, we tested whether high exogenous [P_i] decreased the rate of change of the fluorescence signal that we interpret to be due to apparent displacement of ADP by ATP. Hsc70 was initially incubated with 11.5 μM MgADP and 0.5 mM potassium phosphate (pH was adjusted to 7.0); from previous results we would estimate that at this [P_i], approximately half the Hsc70−MgADP complex would have P_i bound (Ha & McKay, 1994). Under this condition, the ATP-induced fluorescence change, when analyzed with a single exponential, has a rate 0.015 ± 0.001 s^{-1}. (Strictly speaking, analysis with a single exponential is an oversimplification, since the fraction of molecules that have P_i bound initially should display biphasic kinetics due to the ordered dissociation of P_i, followed by ADP. However, a more complex analysis of the kinetics is not warranted by the data.) The slower change of fluorescence, which we infer corresponds to a slower release rate of ADP in the presence of P_i, is consistent with (i) the observed fluorescence change being due to ATP binding after ADP release and (ii) ordered release of products prior to ATP binding.

Nucleotide-Induced Fluorescence Changes in an Extended Time Domain for Hsc70. Since the Hsc70 ATPase cycle requires ~10 min at 25 °C (Ha & McKay, 1994), fluorescence was monitored over 30 min, a time span significantly longer than the enzymatic cycle time, in an effort to correlate changes in fluorescence with specific steps of the enzymatic cycle at 25 °C. To monitor a single turnover of MgATP hydrolysis, a slightly less than stoichiometric amount of MgATP (2.1 μM) was mixed with protein (2.5 μM); under these conditions, essentially all nucleotide will be bound to protein. Reducing [ATP] by half did not affect the value of the observed rate of fluorescence change (data not shown). Depending on which wavelength is chosen, the polarity of the fluorescence signal change after ATP binding is different;

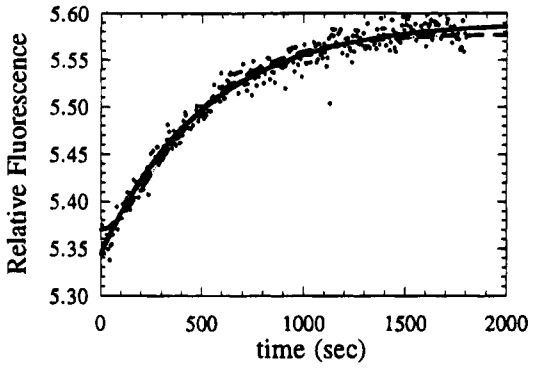

FIGURE 5: Kinetics of the E* → E transition at 25 °C. Hsc70 (2.5 μM) was mixed with a substoichiometric amount of ATP (2.1 μM), and the increase of fluorescence was monitored at 305 nm over 30 min. The solid curve represents a nonlinear least-squares fit of a single exponential. The dashed curve represents a nonlinear least-squares fit of the function with two time-dependent exponential terms, using the rate of chemical hydrolysis determined in Ha and McKay (1994) as one rate constant as described in the text.

at 320 nm, the fluorescence signal decreases, indicating that MgADP quenches more than MgATP, while at 305 nm the fluorescence increases, indicating that the relative quenching is reversed at this wavelength. This agrees with the steady-state emission spectra of Hsc70 bound to different adenine nucleotides. The time course of fluorescence at 305 nm can be approximated with a single exponential with an apparent rate constant 0.00150 ± 0.00002 s^{-1} (Figure 5); the value of the rate constant determined with data collected at 320 nm agrees within experimental error. This rate is substantially slower than that of chemical hydrolysis of ATP (0.0030 ± 0.0003 s^{-1}), suggesting that the observed change correlates with a step after chemical hydrolysis, rather than with hydrolysis itself.

The fluorescence data were therefore fit with a double exponential function in which one constant is equal to the rate of hydrolysis:

$$\text{fluorescence} = A\left[1 - \frac{k_2 e^{-(k_{obs}t)} - k_{obs} e^{-(k_2 t)}}{k_2 - k_{obs}}\right] + C \quad (1)$$

where A is the fluorescence amplitude, C is the offset, and the rate of chemical hydrolysis is k_2 of Scheme 1. Then, the second rate constant has a value 0.0045 ± 0.0010 s^{-1}, which can be compared to the rate constant previously reported for P_i release, 0.0038 ± 0.0010 s^{-1} (k_3 of Scheme 1). It should be noted that, since ADP dissociates rapidly after P_i, these measurements cannot distinguish between the fluorescence change correlating with P_i release versus ADP release, they only distinguish between product release and hydrolysis.

Binding of MgATP and MgADP to the 60 kDa Fragment. Mixing MgATP with nucleotide-free 60 kDa fragment protein produces an initial rapid (time span <0.2 s) decrease in fluorescence, followed by a slower and larger increase over a time span >1 s; the kinetics of MgATP binding to the 60 kDa fragment show the same biphasic behavior that is observed with Hsc70. As was the case with Hsc70, the amplitudes of both phases are temperature-dependent (Figure 6a), precluding accurate measurements of the amplitude of the initial fast phase at $T \geq 25$ °C. Measurements at lower temperatures demonstrated that the apparent rate constant

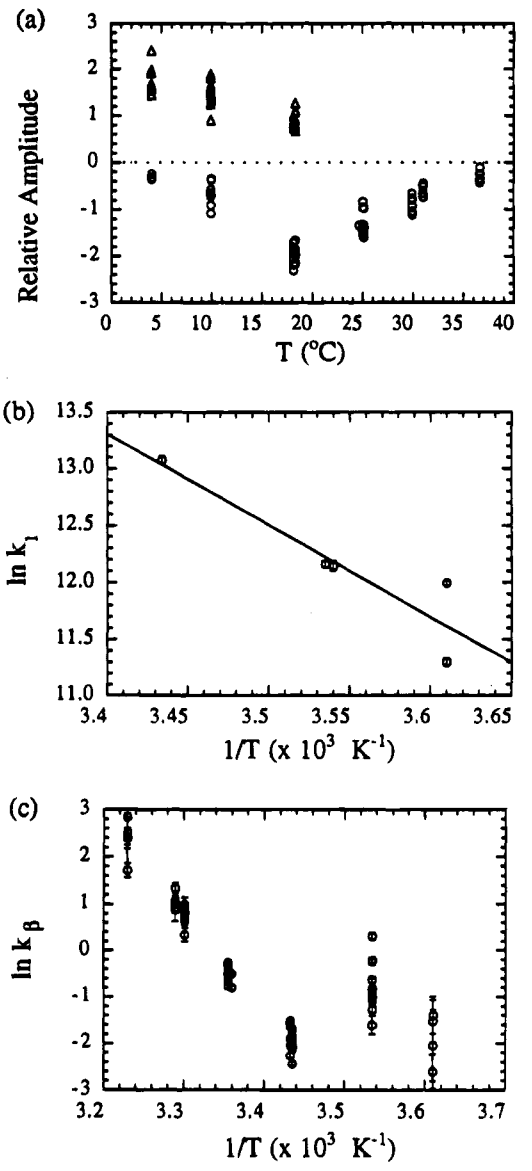

FIGURE 6: Temperature dependence of amplitudes and rate constants of fluorescence changes when MgATP binds to the 60 kDa fragment. (a) (△) The amplitude of the fast phase. (○) The amplitude of the slow phase. (b) Arrhenius plot of the apparent bimolecular association rate constant, k_1. (c) Arrhenius plot of the rate constant of the slower phase, k_β.

of the fast phase has a linear dependence on [ATP], as expected for a bimolecular association reaction. The relative magnitude of the fluorescence change during the second step is approximately 4% at 25 °C. Data collected from 0.5 to 10 s can be fit with a single exponential. The value of the rate constant determined in this manner, 0.63 ± 0.04 s^{-1}, is independent of [ATP] over the range 6.5−190 μM, and is equal within experimental error to the rate of the second step of ATP-induced fluorescence change for Hsc70. Thus, MgATP binding to the 60 kDa fragment induces two sequential changes in fluorescence similar to MgATP binding to Hsc70.

We measured the rate constants of the ATP-induced fluorescence changes over the temperature range 4−37 °C for the slow phase, but only over 4−18 °C for the initial, rapid, phase, due to the small amplitude of the latter at higher temperature. The rate constant of the initial phase, which we infer to correspond to initial binding (k_1 of Scheme 1),

increases approximately 4-fold between 4 and 18 °C (Figure 6b). The apparent activation energy for this step, calculated from the slope of an Arrhenius plot, is 16 ± 4 kcal mol^{-1}. Extrapolation of the linear relationship between ln k_1 and $1/T$ gives a rate constant ~8 × 10^5 M^{-1} s^{-1} at 25 °C.

The apparent [ATP]-independent rate of the second step shows a more complicated temperature dependence. Over the range 18−37 °C, an Arrhenius plot of the data is well fit with a straight line, the slope of which corresponds to an activation energy of 40 ± 1 kcal mol^{-1} (Figure 6c), identical to the value for Hsc70. At lower temperatures, the data deviate from the linear fit of the higher temperatures, suggesting that alternative, or more complex, processes may contribute to the observed fluorescence changes below 18 °C.

MgADP binding quenches tryptophan fluorescence of the 60 kDa fragment approximately 8% at 25 °C (data not shown). The decrease of the signal follows a single exponential, and the apparent association rate increases linearly with increasing [ADP] over the range 28−116 μM. The bimolecular association rate constant of MgADP is (1.3 ± 0.1) × 10^6 M^{-1} s^{-1} which is estimated from the linear fit with a zero intercept to k_{obs}. Floating the intercept does not change the computed value of the bimolecular association rate constant beyond experimental error.

The fluorescence of the 60 kDa fragment was also monitored on an extended time scale after mixing stoichiometric amounts of ATP and nucleotide-free protein at 25 °C. The decrease in fluorescence can be fit with a single exponential with a rate constant 0.0016 ± 0.0001 s^{-1}. For the 60 kDa fragment, kinetic experiments have shown that ATP hydrolysis is the rate-limiting step of the ATPase cycle, and that its rate is 0.0017 ± 0.0001 s^{-1} at 25 °C (Wilbanks et al., 1995). Product release (both P_i and ADP) follows rapidly after hydrolysis. Consequently, the kinetic effect of hydrolysis cannot be readily distinguished from that of product release for reactions triggered synchronously by the addition of ATP. The fluorescence measurements show that the change on the extended time scale correlates with ATP hydrolysis/product release, which is not inconsistent with the results discussed above of similar experiments on Hsc70.

In summary, the observed kinetics of the fluorescence changes of the 60 kDa fragment parallel those of Hsc70: ATP binding is biphasic, and the kinetic constants and activation energies are similar for Hsc70 and the 60 kDa fragment (Table 1); ADP binding is a single-step, second-order process. Observation over a single cycle of ATPase activity shows a fluorescence change which correlates with product release in Hsc70 and ATP hydrolysis/product release in the 60 kDa fragment.

Binding of MgATP and MgADP to the 44 kDa ATPase Fragment. MgATP and MgADP, when mixed with nucleotide-free ATPase fragment protein, quench tryptophan fluorescence approximately 8 and 6%, respectively (data not shown). To determine binding kinetics of the nucleotides, as monitored by the fluorescence, the apparent rate of fluorescence change was measured as a function of nucleotide concentration at 25 °C. The time dependence of the fluorescence decrease following rapid mixing of nucleotides with protein is well fit with a single exponential. The observed rate constant, k_{obs}, increases linearly with increasing nucleotide concentration for both MgATP and MgADP.

Table 1: Kinetic Parameters for the Association of MgATP and MgADP[a]

	parameter	fluorescence[b]	filter binding[c]
Hsc70	k_1 (M^{-1} s^{-1})	~7 × 10^5 [e]	nd[d]
	k_β (s^{-1})[f]	0.68 ± 0.02	nd[d]
	k_{-4} (M^{-1} s^{-1})	(11 ± 1) × 10^5	(4.1 ± 0.5) × 10^5
	k_4 (s^{-1})	0.022 ± 0.002	0.0288 ± 0.0018
60 kDa	k_1 (M^{-1} s^{-1})	~8 × 10^5 [e]	nd[d]
	k_β (s^{-1})[f]	0.63 ± 0.04	nd[d]
	k_{-4} (M^{-1} s^{-1})	(13 ± 1) × 10^5	nd[d]
44 kDa	k_1 (M^{-1} s^{-1})	(3.2 ± 0.2) × 10^5	nd[d]
	k_{-4} (M^{-1} s^{-1})	(5.9 ± 0.3) × 10^5	(3.7 ± 0.5) × 10^5

[a] Parameters are defined in the text. [b] Values were determined at 25 °C in 40 mM HEPES, 4.5 mM $Mg(OAc)_2$, and 75 mM KCl, adjusted to pH 7.0 using the stopped-flow fluorescence technique. [c] Previously determined value at 25 °C in 40 mM HEPES, 4.5 mM $Mg(OAc)_2$, 75 mM KCl, and 50 μg/mL bovine serum albumin, adjusted to pH 7.0. Published in Ha and McKay (1994). [d] Not determined. [e] This value was computed from the apparent activation energy calculated from k_1 determined at temperatures in the range of 4−18 °C for the 60 kDa fragment and the range of 3.1−18.5 °C for Hsc70. [f] [ATP]-independent rate constant ($\approx k_1^* + k_{-1}^*$).

MgATP and MgADP therefore bind to the 44 kDa fragment in a single-step, bimolecular association reaction.

For MgADP, the slope of a straight line fit to k_{obs} versus [ADP] (equal to the bimolecular association rate constant, k_{-4} of Scheme 1) is (5.0 ± 0.5) × 10^5 M^{-1} s^{-1} and the intercept is 35 ± 13. The ADP dissociation rate constant (k_4 of Scheme 1) for the 44 kDa fragment was earlier measured to be 0.0347 ± 0.0016 s^{-1} with a filter binding assay (Ha & McKay, 1994). When the intercept is fixed to 0.0347 s^{-1} (≈0 on the scale of the experimental parameters here), the slope of the linear fit is (5.9 ± 0.3) × 10^5 M^{-1} s^{-1}. This value can be compared to, and is in reasonable agreement with, the value of k_{-4} determined in previous kinetic experiments, (3.7 ± 0.5) × 10^5 M^{-1} s^{-1}.

For MgATP, the slope of a linear fit (equal to k_1 of Scheme 1, since we do not observe a second transition) is (2.7 ± 0.5) × 10^5 M^{-1} s^{-1} and the intercept is 28 ± 25. If the intercept is fixed at zero, the bimolecular association rate constant calculated from a linear fit is (3.2 ± 0.2) × 10^5 M^{-1} s^{-1}. For both nucleotides, when the intercept is set equal to either the value determined by independent experiments or zero, the estimated bimolecular association rate constants are similar to those calculated with the intercept unconstrained.

DISCUSSION

We have examined the kinetics of changes in tryptophan fluorescence resulting from interaction of MgATP and MgADP with recombinant bovine Hsc70 and subfragments thereof, the 60 kDa and 44 kDa fragments. We have used stopped-flow fluorescence techniques to monitor changes on the time scale of nucleotide binding (0.001−20.0 s), and conventional fluorescence techniques to monitor changes on the scale of the cycle time of the ATPase reaction (10^2−10^3 s). Previously we used pre-steady-state kinetics to determine the rate constants of the individual enzymatic steps of the ATPase cycle (Ha & McKay, 1994); however, these studies were not sensitive to multiple conformations of Hsc70 (Scheme 1). Two different conformational states have been identified for Hsc70 and the 60 kDa fragment by solution small-angle X-ray scattering (Wilbanks et al., 1995);

Scheme 2

$$E + ATP \underset{k_{-1}}{\overset{k_1}{\rightleftharpoons}} E\text{–}ATP \underset{k^*_{-1}}{\overset{k^*_1}{\rightleftharpoons}} (E\text{–}ATP)^*$$

Scheme 3

$$E + ATP \underset{k^*_{-1}}{\overset{k^*_1}{\rightleftharpoons}} E^* + ATP \underset{k_{-1}}{\overset{k_1}{\rightleftharpoons}} (E\text{–}ATP)^*$$

Scheme 4

$$E\text{–}ATP \underset{k_{-1}}{\overset{k_1}{\rightleftharpoons}} E + ATP \underset{k^*_{-1}}{\overset{k^*_1}{\rightleftharpoons}} (E\text{–}ATP)^*$$

these appear to be the high-peptide-affinity and low-peptide-affinity states of the proteins. However, the time scale of SAXS measurements (~1−2 min) is too coarse to monitor changes between the two different conformations on the time scale of nucleotide binding. The focus of this study is to correlate the kinetics of nucleotide-induced changes in tryptophan fluorescence with kinetics of the enzymatic ATPase cycle, and then to infer which steps of, or associated with, the ATPase cycle may correlate with conformational changes of Hsc70.

ADP binding to Hsc70, the 60 kDa fragment, or the 44 kDa fragment generates a rapid single-step change in fluorescence whose observed rate constant increases linearly with nucleotide concentration. The bimolecular association rate constants, derived from the fluorescence data, are in approximate agreement with ADP association rates measured directly by filter binding (Table 1). By implication, the ADP-induced change in fluorescence appears to monitor nucleotide binding, which appears to be a one-step, bimolecular process.

In contrast, ATP binding to Hsc70 or the 60 kDa fragment induces a two-step fluorescence change. The observed rate of the first step increases linearly with nucleotide concentration, while the rate of the second step is concentration-independent. It is notable that the rate of the second transition (~0.7 s^{-1} at 25 °C) is 2 orders of magnitude faster than the rate of hydrolysis (~0.003 s^{-1} at 25 °C), so that hydrolysis does not obscure the kinetics of the binding processes and can be ignored in the analysis.

Biphasic kinetics with these characteristics can, theoretically, originate from three different mechanisms (Halford, 1972; Bagshaw et al., 1974; Johnson, 1992): initial bimolecular association followed by a rearrangement of the complex (Scheme 2, where "E" may represent either Hsc70 or the 60 kDa fragment); interconversion between two conformations of the protein alone, with ligand binding to only one form of the protein (Scheme 3); or a mechanism involving two distinct ligand binding modes (Scheme 4). In Scheme 3, the protein would interconvert between two different forms in the absence of the nucleotide, only one of which would bind ATP. If there is a difference in fluorescence between E* and (E−ATP)*, then the fluorescence kinetics will be biphasic, with one rate constant due to binding of ATP to E* (a second-order process), and the other due to interconversion between E and E* (a first-order process). To give single-step kinetics for ADP binding, an additional constraint on this scheme would be that the equilibrium between unligated protein states lies far in the direction of E, and that ADP binds only to E, not E*. Otherwise, ADP binding would also have biphasic kinetics. Consequently, this model requires that Hsc70 and the 60 kDa fragment interconvert between two states which are mutually exclusive in their nucleotide binding properties; E* would bind ATP but not ADP, while the converse would be true for E. Although theoretically possible, such a process, whereby conformational changes in the protein differentiate nucleotide binding, rather than nucleotide binding inducing conformational changes, seems unlikely.

Scheme 4, under restricted conditions, can also result in biphasic kinetics of the type we observe. For example, if ATP binds rapidly in two different ways but is released rapidly from one complex, E−ATP, but slowly from the other, (E−ATP)*, then after initial binding, flux of ATP from E−ATP to (E−ATP)* will appear first-order under conditions where release of ATP from the former complex determines the overall rate. This would require a fortuitous constellation of conditions to give the results observed with ATP binding, in addition to requiring two different ATP binding modes.

Scheme 2 involves two sequential steps: bimolecular association of MgATP with Hsc70 (a second-order process), followed by a first-order process, possibly a conformational change of the Hsc70−MgATP complex. The rates of change of concentrations of E, E−ATP, and (E−ATP)* are then functions of two rate constants, which we denote k_α and k_β (Johnson, 1986, 1992); in the case that $k_\beta \ll k_\alpha$, the constants can be approximated:

$$k_\alpha = k_1[ATP] + k_{-1} + k^*_1 + k^*_{-1} \quad (2)$$

$$k_\beta = \{k_1[ATP](k^*_1 + k^*_{-1}) + k_{-1}k^*_{-1}\}/k_\alpha \quad (3)$$

In this approximation, k_α is linearly dependent on [ATP] with a slope of k_1. The general solution for the time dependence of [E−ATP] is a function which has two exponential terms with rate constants k_α and k_β; at times small compared to $1/k_\beta$, the term with rate k_α dominates, resulting in an observed rate constant whose value increases linearly with substrate concentration, with a slope k_1. In a similar vein, the general solution for (E−ATP)* as a function of time also has two exponential terms; at times large compared to $1/k_\alpha$, the k_β term dominates. At sufficiently high [ATP], the asymptotic value of k_β equals $k^*_1 + k^*_{-1}$; the observed rate constant for (E−ATP)* formation becomes concentration-independent.

Consequently, we favor Scheme 2—where MgATP binds protein; then the ATP−protein complex rearranges—as the model with which to interpret our data of MgATP binding to Hsc70 and the 60 kDa fragment. The conditions under which the second step of the process is observed—with MgATP binding in the presence of K^+, but not with MgADP, not with MgAMP−PNP, and not with MgATP in the presence of Na^+—are the conditions under which Hsc70 is known to undergo a conformational change from the high-peptide-affinity state to the low-peptide-affinity state. Hence, it is reasonable to suggest that the second step of the MgATP binding process seen by fluorescence monitors the conformational change that induces peptide release in Hsc70.

Previously we measured the rate of MgATP binding to Hsc70 at 25 °C with a limiting [ATP] of 1 nM and [Hsc70] ranging 22 −160 nM using a filter binding assay (Ha & McKay, 1994). The observed rate of ATP binding increased

linearly with [Hsc70]; the slope and intercept of the linear fit were (2.7 ± 0.5) × 10^5 M^{-1} s^{-1} and 0.0114 ± 0.0002 s^{-1}, respectively. In the context of the two-step binding process suggested by fluorescence, these numbers can be interpreted as follows. The time scale of the sampling for filter binding was tens of seconds, substantially longer than the time required for the E−ATP → (E−ATP)* transition after binding. In the [Hsc70] range where the filter binding was performed, k_1[Hsc70] ≪ $k_1^* + k_{-1}^*$, and the major complex retained on the filter is (E−ATP)*. When, $k_1^* \gg k_{-1}^*$, the fraction of Hsc70 in the (E−ATP)* state will be determined by the apparent equilibrium constant, $K_d^1 K_d^*$, where K_d^1 and K_d^* are the equilibrium dissociation constant of the bimolecular association step and the conformational isomerization step, respectively. In addition, the concentration of (E−ATP)* is determined predominantly by k_β. Then, for a linear fit of the observed binding rate (k_β) versus [Hsc70] at low Hsc70 concentration (Johnson, 1992):

$$\text{slope} \approx \frac{k_1(k_1^* + k_{-1}^*)}{k_{-1} + k_1^* + k_{-1}^*} \quad (4)$$

$$\text{intercept} \approx \frac{k_{-1}k_{-1}^*}{k_{-1} + k_1^* + k_{-1}^*} \quad (5)$$

Using eqs 4 and 5, as well as values of k_1 (~7 × 10^5 M^{-1} s^{-1}) and $k_1^* + k_{-1}^*$ (0.68 s^{-1}; this work), values for the three remaining rate constants at 25 °C can be estimated: $k_{-1} \approx$ 1.1 s^{-1}; $k_{-1}^* \approx$ 0.02 s^{-1}; $k_1^* \approx$ 0.66 s^{-1}. MgATP therefore binds to Hsc70 with a two-step mechanism in which the initial, relatively weak binding ($K_d^1 \approx 1.5$ μM) is followed by a conformational change ($K_d^* \approx 0.03$) leading to a tighter ATP complex ($K_d^1 K_d^* = 0.042 \pm 0.007$ μM). In addition, initial MgATP binding is not in rapid equilibrium (since $k_{-1} \approx k_1^*$), and the equilibrium of the second step of MgATP binding to Hsc70 is far to the right ($k_1^* \gg k_{-1}^*$).

When a stoichiometric amount of ATP is mixed with Hsc70 under single turnover conditions and the fluorescence is monitored over an extended time, the kinetics of the response correlate with the kinetics of product release; they are substantially slower than hydrolysis. Since product release is ordered, with ADP dissociating rapidly after P_i, the response does not distinguish between the two dissociation steps. When a stoichiometric amount of ATP is mixed with the 60 kDa fragment, release of both products (P_i, followed by ADP) is relatively rapid after hydrolysis. When the fluorescence is monitored under these conditions, the kinetics of the response correlate with the rate of ATP hydrolysis/product release; the results on the 60 kDa fragment are consistent with those on Hsc70, although they cannot discriminate hydrolysis from product release.

The kinetic framework of the Hsc70 ATPase cycle can now be augmented to incorporate the results of the tryptophan fluorescence studies, which we infer to monitor nucleotide binding and nucleotide-induced conformational changes (Scheme 5). (Strictly speaking, we should have an "E" state and an "E*" state for each step of the ATPase cycle. However, for the sake of simplicity, we are showing only the significantly populated states of the more general scheme.) Initial ATP binding is a bimolecular process, and

Scheme 5

$$\text{E} + \text{ATP} \underset{k_{-1}}{\overset{k_1}{\rightleftharpoons}} \text{E–ATP} \underset{k_{-1}^*}{\overset{k_1^*}{\rightleftharpoons}} \text{(E–ATP)*} \xrightarrow{k_2}$$

$$\text{(E–ADP–P}_i\text{)*} \underset{k_{-3}}{\overset{k_3}{\rightleftharpoons}} \begin{matrix}\text{E–ADP + P}_i \\ \text{or} \\ \text{(E–ADP)* + P}_i\end{matrix} \underset{k_{-4}}{\overset{k_4}{\rightleftharpoons}} \text{E + ADP + P}_i$$

is significantly slower than diffusion-limited binding, which would have k_{on} ~10^8−10^9 M^{-1} s^{-1}. The temperature dependence of the rate constant gives an activation energy of ~14 kcal mol^{-1} for this step. The second step is a first-order process which we interpret to be a conformational change. Since $k_1^* \gg k_{-1}^*$, the measured rate constant of this step, k_β, is approximately equal to k_1^*; it follows that the Arrhenius plot of the temperature dependence of k_β, which has a slope of 40 kcal mol^{-1} (Figure 3c), gives an estimate of the activation energy for the conformational change.

The reverse transition, E* → E, is induced by product release. We have not been able to drive Hsc70 in the opposite direction, E → E*, by addition of ADP; this suggests that E−ADP is stable, and that P_i release drives the transition. However, we have not succeeded in driving Hsc70 from E to E* by adding P_i to a Hsc70−ADP complex. It may be the case that a (Hsc70−ADP−P_i)* state is kinetically inaccessible by the reverse route under the conditions we have tried, in view of the relatively slow binding (10^2−10^3 M^{-1} s^{-1}) and weak affinity (K_d ~ 1 mM) of P_i for the complex (Ha & McKay, 1994). Alternatively, the product release that induces the E* → E transition may, theoretically, be a two-step process, with the first step being essentially irreversible, so that the reverse transition E → E* will be inaccessible from the route of rebinding product.

The 60 kDa fragment appears to mimic Hsc70 in this cycle. In particular, the kinetic constants for binding and release of nucleotides from the 60 kDa fragment are almost identical to those of Hsc70 (Table 1). In contrast, the 44 kDa ATPase fragment (which lacks the peptide binding domain) does not show biphasic kinetics when ATP binds; we have found no evidence for a substantial conformational change in this fragment of the type observed in Hsc70 and the 60 kDa fragment.

A question which arises is what, at the molecular level, the E* state is. Nucleotide binds at the base of a cleft in Hsc70, so it might be suggested that the E → E* transition is the cleft closing onto the nucleotide after initial binding. However, since the transition is seen only with MgATP in the presence of K^+, and not with other nucleotides that are known to bind (MgADP; MgAMP−PNP), it seems unlikely that cleft closure is the source of the transition.

Although the 44 kDa ATPase fragment does not show the same ATP-induced conformational change as Hsc70, it is instructive to discuss available information on the interactions of nucleotides with this fragment, with the caveat that Hsc70 and the 60 kDa fragment must have additional (direct or indirect) interactions that give rise to their more complex behavior. Crystallographic and kinetic studies of wild-type and mutant ATPase fragment proteins have suggested a reaction pathway for ATP hydrolysis in which (1) nucleotide triphosphates (ATP or AMP−PNP) initially bind in a manner such that the nucleotide fails to complex the protein-bound Mg^{2+} tightly; then, after rearrangement of the γ-phosphate of the nucleotide, (2) a tight β,γ-bidentate complex between

Mg^{2+} and phosphate oxygens is formed, while two protein-bound K^+ ions also interact with the terminal phosphates; this intermediate state is then positioned for in-line attack on the γ-phosphate by an H_2O molecule or OH^- ion, resulting in (3) hydrolysis (Wilbanks & McKay, 1995; Flaherty et al., 1994; Wilbanks et al., 1994; O'Brien & McKay 1993). It is reasonable to suggest that the intermediate β,γ-bidentate state, which leads up to the chemical attack on the terminal phosphate and formation of a transition state of the hydrolytic reaction, is a candidate for the nucleotide state that induces the conformational change from the high-peptide-affinity state to the low-peptide-affinity state in Hsc70.

ACKNOWLEDGMENT

We thank Drs. Roger Goody and Jon Goldberg for assistance with the stopped-flow spectrofluorometer, Stanford University Biochemistry Department for use of their stopped-flow spectrofluorometer and luminescence spectrometer, and Dr. Lubert Stryer for the use of his SLM 8000C spectrofluorometer. We gratefully acknowledge Dr. Sigurd Wilbanks for helpful discussions and Lauren Shirvanee, Eugene Golts, and Samina Taha for assistance in purifying the 44 kDa and the 60 kDa fragments.

REFERENCES

Bagshaw, C. R., Eccleston, J. F., Eckstein, F., Goody, R. S., Gutfreund, H., & Trentham, D. R. (1974) *Biochem. J. 141*, 351−364.

Chappell, T. G., Welch, W. J., Schlossman, D. M., Palter, K. B., Schlesinger, M. J., & Rothman, J. E. (1986) *Cell 45*, 3−13.

Chappell, T. G., Konforti, B. B., Schmid, S. L., & Rothman, J. E. (1987) *J. Biol. Chem. 262*, 746−751.

Flaherty, K. M., DeLuca-Flaherty, C., & McKay, D. B. (1990) *Nature 346*, 623−628.

Flaherty, K. M., Wilbanks, S. M., DeLuca-Flaherty, C., & McKay, D. B. (1994) *J. Biol. Chem. 269*, 12899−12907.

Gao, B., Greene, L., & Eisenberg, E. (1994) *Biochemistry 33*, 2048−2054.

Gething, M. J., & Sambrook, J. (1992) *Nature 355*, 33−45.

Ha, J.-H., & McKay, D. B. (1994) *Biochemistry 33*, 14625−14635.

Halford, S. E. (1972) *Biochem. J. 126*, 727−738.

Hightower, L. E., Sadis, S. E., & Takenaka, I. M. (1994) in *The Biology of Heat Shock Proteins and Molecular Chaperones*, pp 179−208, Cold Spring Harbor Laboratory Press, Cold Spring Harbor, NY.

Johnson, K. A. (1986) *Methods Enzymol.*, 677−705.

Johnson, K. A. (1992) in *The Enzymes*, pp 1−61, Academic Press Inc., New York.

Liberek, K., Skowyra, D., Zylicz, M., Johnson, C., & Georgopoulos, C. (1991) *J. Biol. Chem. 266*, 14491−14496.

McKay, D. B. (1993) *Adv. Protein Chem. 44*, 67−98.

McKay, D. B., Wilbanks, S. M., Flaherty, K. M., Ha, J.-H., O'Brien, M. C., & Shirvanee, L. L. (1994) in *The Biology of Heat Shock Proteins and Molecular Chaperones*, pp 153−177, Cold Spring Harbor Laboratory Press, Cold Spring Harbor, NY.

Morshauser, R. C., Wang, H., Flynn, G. C., & Zuiderweg, E. R. P. (1995) *Biochemistry 34*, 6261−6266.

O'Brien, M. C., & McKay, D. B. (1993) *J. Biol. Chem. 268*, 24323−24329.

Palleros, D. R., Reid, K. L., McCarty, J. S., Walker, G. C., & Fink, A. L. (1992) *J. Biol. Chem. 267*, 5279−5285.

Palleros, D. R., Reid, K. L., Shi, L., Welch, W. J., & Fink, A. L. (1993) *Nature 365*, 664−666.

Perrin, D. D., & Dempsey, B. (1974) *Buffers for pH and Metal Ion Control*, John Wiley & Sons, New York.

Prasad, K., Heuser, J., Eisenberg, E., & Greene, L. (1994) *J. Biol. Chem. 269*, 6931−6939.

Schlossman, D. M., Schmid, S. L., Braell, W. A., & Rothman, J. E. (1984) *J. Cell Biol. 99*, 723−733.

Schmid, S. L., & Rothman, J. E. (1985) *J. Biol. Chem. 260*, 10044−10049.

Tonomura, B., Nakatani, H., Ohnishi, M., Yamaguchi-Ito, J., & Hiromi, K. (1978) *Anal. Biochem. 84*, 370−383.

Wang, T., Chang, J., & Wang, C. (1993) *J. Biol. Chem. 268*, 26049−26051.

Wilbanks, S. M., & McKay, D. B. (1995) *J. Biol. Chem. 270*, 2251−2257.

Wilbanks, S. M., DeLuca-Flaherty, C., & McKay, D. B. (1994) *J. Biol. Chem. 269*, 12893−12898.

Wilbanks, S. M., Chen, Tsuruta, Hodgson, & McKay (1995) *Biochemistry* (in press).

BI9511144